Commissioning and quality assurance of a novel solution for respiratory-gated PBS proton therapy based on optical tracking of surface markers

Giovanni Fattori[a,*], **Jan Hrbacek**[a], **Harald Regele**[a], **Christian Bula**[a], **Alexandre Mayor**[a], **Stefan Danuser**[a], **David C. Oxley**[a], **Urs Rechsteiner**[a], **Martin Grossmann**[a], **Riccardo Via**[a], **Till T. Böhlen**[a], **Alessandra Bolsi**[a], **Marc Walser**[a], **Michele Togno**[a], **Emma Colvill**[a], **Daniel Lempen**[a], **Damien C. Weber**[a,b,c], **Antony J. Lomax**[a,d], **Sairos Safai**[a]

[a] Center for Proton Therapy, Paul Scherrer Institute, 5232 Villigen, Switzerland
[b] Department of Radiation Oncology, University Hospital Zurich, 8091 Zurich, Switzerland
[c] Department of Radiation Oncology, University Hospital Bern, 3000 Bern, Switzerland
[d] Department of Physics, ETH Zurich, 8092 Zurich, Switzerland

Received 21 February 2020; accepted 10 July 2020

Abstract

We present the commissioning and quality assurance of our clinical protocol for respiratory gating in pencil beam scanning proton therapy for cancer patients with moving targets. In a novel approach, optical tracking has been integrated in the therapy workflow and used to monitor respiratory motion from multiple surrogates, applied on the patients' chest. The gating system was tested under a variety of experimental conditions, specific to proton therapy, to evaluate reaction time and reproducibility of dose delivery control. The system proved to be precise in the application of beam gating and allowed the mitigation of dose distortions even for large (1.4 cm) motion amplitudes, provided that adequate treatment windows were selected. The total delivered dose was not affected by the use of gating, with measured integral error within 0.15 cGy. Analysing high-resolution images of proton transmission, we observed negligible discrepancies in the geometric location of the dose as a function of the treatment window, with gamma pass rate greater than 95% (2%/2 mm) compared to stationary conditions. Similarly, pass rate for the latter metric at the 3%/3 mm level was observed above 97% for clinical treatment fields, limiting residual movement to 3 mm at end-exhale. These results were confirmed in realistic clinical conditions using an anthropomorphic breathing phantom, reporting a similarly high 3%/3 mm pass rate, above 98% and 94%, for regular and irregular breathing, respectively. Finally, early results from periodic QA tests of the optical tracker have shown a reliable system, with small variance observed in static and dynamic measurements.

Keywords: Proton therapy, Moving tumours, Respiratory gating, Optical tracking, Surface markers, Commissioning, Quality assurance

* Corresponding author: Giovanni Fattori, Paul Scherrer Institut, 5232 Villigen, Switzerland.
E-mail: giovanni.fattori@psi.ch (G. Fattori).

Z Med Phys **32** (2022) 52–62
https://doi.org/10.1016/j.zemedi.2020.07.001
www.elsevier.com/locate/zemedi

1 Introduction

Intensity modulated radiotherapy treatments make use of sharp dose gradients to limit the radiation damage to the cancer area, preserving surrounding healthy tissues. High precision however comes with an increased sensitivity to anatomical uncertainties and organ motion, challenging the quality of conformal treatments in sites affected by respiratory motion. Several strategies have been proposed for effective motion mitigation in particle therapy [1], among which rescanning [2] and respiratory gating [3,4] were recently introduced in clinical protocols at several institutes.

Monitoring the breathing motion is therefore crucial in radiotherapy treatments of thoracic tumours and similarly the foundation of many techniques for time resolved imaging [5]. This important role notwithstanding, many commonly used devices provide only a simplified representation of the actual dynamic patient geometry, which limits their potential in high-precision radiotherapy applications. That is the case for load cell sensors [6], distance meters [7] and early video-based methods [8], measuring a surrogate signal from a single point, often in arbitrary units. As an alternative, we propose a novel solution for the accurate measurement of body surface displacement based on optical tracking and report on the commissioning activities that preceded its clinical integration for respiratory-gated proton therapy treatments.

Optical tracking systems based on stereo-photogrammetric localisation of markers are reference technologies for surgical navigation and motion monitoring in radiotherapy, providing high accuracy measurements with a minimally invasive setup for image-guided interventions. That is also true for proton therapy applications [8–10], where optical methods are shown to outperform the major alternative based on electromagnetic tracking [11], for reliability and robustness against environmental distortions [12].

One of the most popular products is the Real-Time Position Management System (RPM) commercialised by Varian Medical Systems (Palo Alto, CA, USA), recently updated to its new version – RGSC [13], using a single camera to localise a reflector block on the patient's abdomen. More sophisticated tracking solutions however combine the signals from stereo cameras to measure with high accuracy the body surface [14] or the position of individual markers distributed on the thorax [15,16]. That approach is supported by several studies discussing the benefit of the use of redundant surface points to improve image reconstruction [17] and motion modelling [18,19]. Applied in photon radiotherapy for years, optical tracking of multiple surrogates however has seen limited adoption in proton therapy. Its use is documented for patient positioning and setup verification [20–22] but the clinical adoption for real time motion monitoring and beam gating in proton therapy has not yet been reported outside experimental applications [23,24].

In particular, pencil beam scanned (PBS) proton therapy, whilst allowing for high precision dose painting, is highly sensitive to uncertainties due to organ motion when compared to conventional radiotherapy [1,25]. Here, we present the methods and results of the clinical commissioning and quality assurance program of our customised solution for real-time motion monitoring in respiratory-gated pencil beam scanning (PBS) proton therapy.

2 Materials and methods

2.1 Monitoring motion from body markers

Breathing motion is monitored by tracking the position of a configuration of six body markers placed on the patient torso in a standardised configuration as described in Fig. 1 (left panel). Aiming for a simplified workflow, anatomic landmarks such as xiphoid, umbilicus or the sternal angle points, are used as reference, thus avoiding the skin tattoos typically used in radiotherapy. All points are measured simultaneously, to quantify the deformation of different body regions at the same time, from the lower abdomen to the upper thorax. In this first implementation, only anterior-posterior motion is monitored, by following an initial calibration procedure to map OTS data to the local reference system of the couch top (Fig. 1 – right panel).

The gating window is specified for each marker individually, as a percent of its range of motion. To translate the amplitude percent into practice, after immobilisation and setup for radiotherapy, the patient is acquired while free breathing over a defined period of time, typically around 1 min, to calculate the *daily reference parameters*. On this data, inhale and exhale peaks are detected for each available marker trajectory, to measure the motion ranges and the respiratory exhale baseline. The marker with the largest motion is additionally used to calculate the patient's reference breathing period. CT imaging and beam delivery are then triggered, whilst comparing such *daily reference parameters* with the real-time measurements, when all markers fall within the specified gating threshold. In our current clinical protocol, the same gating window is set for all markers at 30% amplitude of the surface motion range. Each marker can be individually disregarded in the gating detection and its threshold individually set, if required by the use case. Our current implementation supports end-exhale treatments; therefore, each gating level is considered as an upper bound.

Radiation is however interrupted if any marker considered for gating shifts below the free-breathing baseline by more than 5% of its respective motion range or the breathing period variability is above 30% of the reference value. These safety thresholds may be subject to change in the future, as we gain clinical experience.

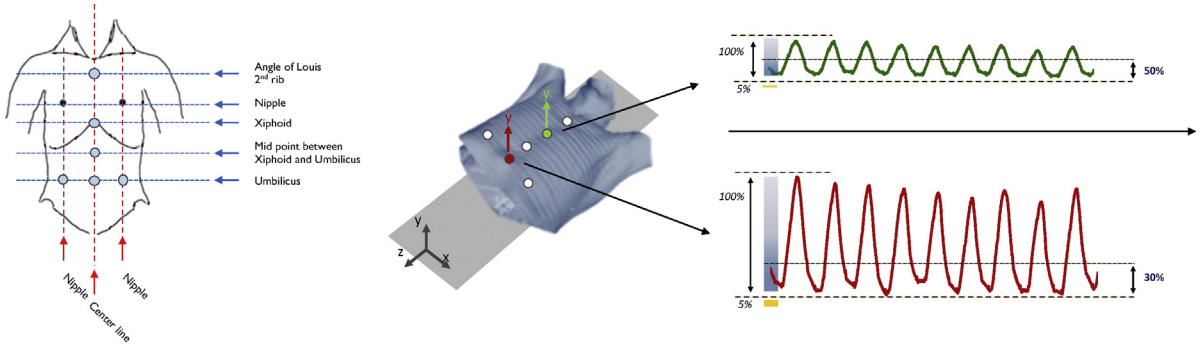

Figure 1. The standard protocol for marker positioning based on anatomical landmarks is shown in the left panel. Body silhouette adapted from [12 – Fig. 1]. On the right, concurrent measurement of respiratory waveform at umbilicus and xiphoid points obtained from a healthy volunteer. Gating window is set respectively at 30% and 50% of the range of motion in an exemplary use case. Tolerance on the baseline shift is set at 5% (yellow bar).

2.1.1 Body markers water equivalent thickness

In the clinical routine, we use non-sterile infrared reflective markers for skin application. Currently, we rely on SORT-A (Atesos Medical AG, Aarau, CH), plastic spheres coated with infrared reflective material and provided with a pad of medical grade acrylic adhesive tested for cytotoxicity, irritation and sensitization. A transparent plastic cover, protecting the reflective element from deterioration, makes these surrogates re-utilisable in the long run. They produce artefact-free radiological images and the water equivalent thickness (WET) of this marker model type has been estimated prior to use in proton therapy.

The marker WET has been measured on proton radiography images taken with a scintillating screen coupled with a CCD camera (Apogee Alta U6, Roseville, US). Radiographic scans were obtained with a homogenous energy layer at 130 MeV, converting CCD pixel intensities into the corresponding energy loss and correcting for quenching effects. Multiple images were acquired and stacked up, progressively offsetting the Bragg peak fall-off with layers of qualified polymethyl methacrylate to scan through the whole object depth. Purpose of this measurement is not to obtain accurate materials data for the treatment planning system but to have a first estimation of the markers homogeneity, and possibly consider the need for specific beam arrangements.

2.2 Clinical workflow for gating

The clinical workflow relies on the availability of the same motion monitoring system at the time of treatment simulation and delivery. For each potential treatment candidate of respiratory gating, both 4D CT and end-exhale prospectively gated CT are acquired and evaluated at an early stage of the planning workflow. The amplitude of target motion observed on 4DCT images, retrospectively binned in amplitude phases using the surface motion signal, is the key parameter to stratify patients, selecting those that would benefit from respiratory gating from others to be treated in free-breathing with rescanning [26]. In the case that gating is necessary, the treatment is planned on the gated CT, using the 4DCT phases within the gating window to draw an internal target volume (ITV). On this latter dataset, the generated plan is also tested for robustness against the residual motion, using 4D dose calculations to scale appropriately the rescanning factor. Patient setup is verified with volumetric image registration between a daily gated-CT acquired with an in-room scanner (Siemens Somatom Sensation Open on-rails, Erlangen, Germany) and the planning image. Imaging may be repeated during the treatment fraction to correct for shifts in the motion baseline and set new tolerance for the lower bound of markers position at end-exhale. Every time new *daily reference parameters* are acquired, automated checks are in place to compare the daily range of motion of surface surrogates against those recorded during the acquisition of the planning CT, and warn the therapist of potential inconsistency in the gating window.

Following the definition of a gating window from multiple surrogates defined in Section 2.1, the actual width of the window, being a function of the daily motion range, may slightly vary over fractions due to patient breathing variability. This uncertainty, together with inter-fraction baseline shifts, are however kept under control by our positioning strategy that requires target-based registration between the planning and daily positioning CT images, both acquired using gating. The ITV, as defined from 4DCT phases within the gating window, is overlaid on the planning CT at time of positioning and used to detect if the daily target motion exceeds the planning margins.

Additionally, control 4DCTs may be acquired during the treatment course to evaluate the consistency of treatment geometry and internal-external correlation.

2.3 Technology integration

The motion monitoring system uses Polaris NDI tracking technology (NDI, Waterloo, CA, USA) to track multiple

points with 0.18 mm (IQR) accuracy and low latency (16.6 ± 1 ms) [12]. The sensor is mounted at the foot end of the couch with a custom holder at an elevation of 50 cm, ensuring clear sight of the patient's thorax for common treatment positions. It connects to the therapy control system and patient safety system through a dedicated beam gating machine interface (BGMI) specifically developed for this application at Center for Proton Therapy. BGMI provides a simple interface to gating signals for the control system that checks for a gate before each spot irradiation and, if required, pauses the delivery until the correct motion state is detected. Based on FPGA logic, the gating interface adds only marginally to the overall reaction time of the system, with latencies of 41.1 ± 6 μs and 50 ± 6 μs measured for signal processing, when entering or exiting the gating window respectively. The same technology is used to communicate with a CT, in our case using the Open Interface of a Siemens Somatom Sensation Open scanner (Erlangen, Germany). Finally, facilitating the retrospective analysis of treatment log files, the motion recorded by the gating system is stored on a shared timestamp with the therapy control system in such a way that it is possible to derive the breathing phase in which each spot is delivered.

2.3.1 Safety measures

The position sensor exceeds by size the clearance boundaries around the treatment couch defined to prevent collisions and patient harm during robotic alignment. The docking of gating equipment is therefore detected and the couch travel modified accordingly, to reduce the risk of collisions. For this purpose, a physical socket on the OTS camera holder is wired with a unique identifier that closes on its counterpart connector (ODU-MAC, ODU GmbH & Co., Mühldorf a. Inn, Germany) in the coupling mechanism. The patient positioning system PLR controller reads the identification socket to set appropriate boundary limits and notifies the therapy control system. In addition, our proprietary machine file format has been extended to include the required equipment, whereas the therapy control system checks for its presence against the requirements specified in the daily treatment fraction.

The BGMI gating interface is a key safety element that monitors the hardware and software functionality. Every new motion frame captured by the gating tracking system, a watchdog timer is reset on successful check of the connection status with the camera sensor, the time elapsed since the last data received and plausibility of detected motion speed. The lower and upper time limits for the watchdog reset are set at 10 ms and 22 ms respectively, outside this range the treatment is automatically interrupted for safety reasons, due to malfunctions of the monitoring system. Being particularly strict, such checks are enforced only when the gating interface is engaged, i.e. when a change on the output signal can result in actual beam delivery. The operator controls such operational state of interface from a graphical user interface but, as ultimate safety measure, a physical button is available in the control room as direct hardware bypass, for an immediate disabling of the interface and beam delivery.

Finally, in an attempt to interrupt the treatment as efficiently as possible, the status of the gating signal is checked only before starting the delivery of each individual spot but not during its actual irradiation. However, a hard time threshold on the gate signal fall off is set such that the patient safety system does independently interrupt the treatment after 100 ms of missing gate.

2.4 Clinical commissioning

In total, 4 major commissioning tests have been performed to transfer the system into clinical operation.

2.4.1 Test 1 – Integrity of dose delivery

Initially, the integrity of the total dose delivered in gated treatments was verified using an array of cross-calibrated ionisation chambers (PTW Octavius 1500 XDR, Freiburg, D) aligned statically at iso-center (Fig. 2a). Using this setup, a homogeneous square energy layer field of 5 cm side length has been delivered repeatedly, under the same experimental conditions, to compare the integral dose measured with and without gating interruptions. The proton fluence across the field was uniform and defined such as to deposit 0.75 Gy at the Bragg peak. The same monoenergetic field at 100 MeV has been verified twice, at two depths 4 cm of water apart in the plateau region. To simulate a realistic breathing signal, the vertical component of a two-axis programmable moving platform (QUASAR^{TM} Respiratory Motion Phantom, Modus Medical Devices, London, Ontario, Canada) has been tracked with the sensor to set the gating window at 30% amplitude of the motion range (Fig. 2).

2.4.2 Test 2 – Gating effectiveness

The same experimental setup was used to evaluate the effectiveness of gating as a function of the residual motion for an exemplary clinical case (Fig. 2a). In this plan, originally prepared for the treatment of a mediastinal lesion, the total dose was made up from two fields that are split respectively in 2 and 4 patches (Fig. 3 – left panel). For this particularly large target, the treatment couch moved within the field to cover approximately 20 cm of longitudinal extension [27]. The dosimeter array was set to follow a $sin^4(t)$ curve with 5 s period moving 5 and 10 mm perpendicular to the primary scanning direction. Gating at 30% of amplitude results in approximately 1.5- and 3-mm residual motion, respectively. The measurement was performed roughly in the middle of the field, at 2.49 cm water equivalent depth by adding 1.5 cm Polymethyl Methacrylate (PMMA) plates on top of the dosimeter. All measurements were compared to those of static delivery using the gamma (γ) evaluation limited to measurement points above 10% of the maximal dose at each respective measurement plane.

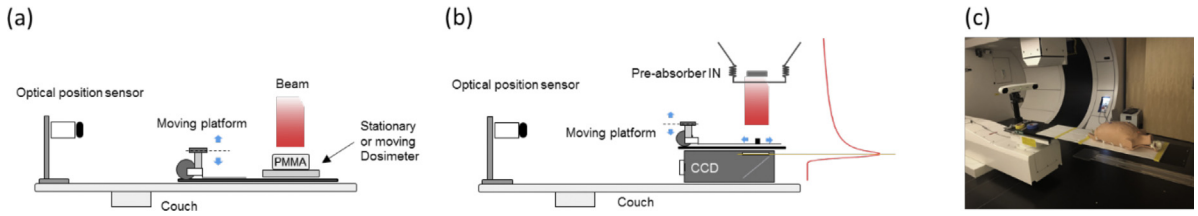

Figure 2. Three experimental setups used for clinical commissioning tests. The optical tracking system is mounted at the end of the robotic table and used to monitor the motion of a variety of moving phantoms and dosimetry devices. From left to right: QUASAR^{TM} moving platform and 2D array of ionization chambers (a), scintillating screen CCD-camera device with QUASAR^{TM} phantom on top (b) and anthropomorphic lung cancer breathing phantom (c).

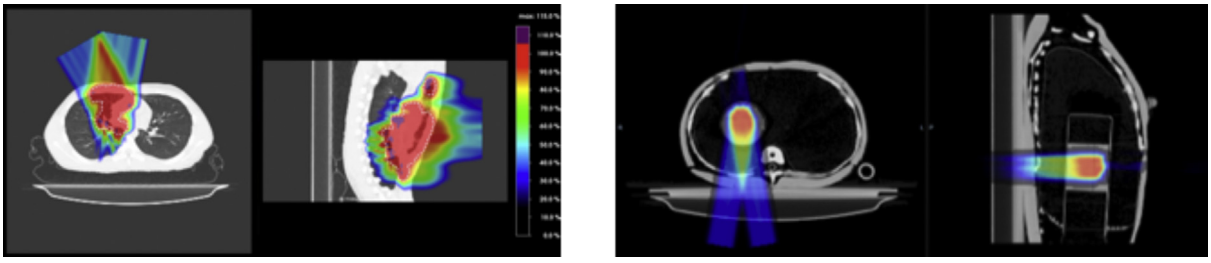

Figure 3. On the left panel a two fields treatment plan optimised for the treatment of a large lesion located in the mediastinal region used in Test 3. On the right, the plan prepared for the end-to-end Test 4 with the anthropomorphic breathing phantom.

2.4.3 Test 3 – Latency and geometric precision

The overall system latency and geometric precision of gating has been assessed on high resolution proton transmission images taken with a scintillating-screen CCD camera device [28] (Figure 2b). In this setup, the QUASAR^{TM} platform has been used to move a solid structure on top of the screen. The CCD camera itself was kept stationary with respect to the beam isocentre. A small polyethylene (PE) block, 3 cm thick, created a sharp shadow on the screen irradiated with a homogeneous energy layer at 100 MeV. The measurement was repeated twice for each combination of sinusoidal target motion ($sin^4(t)$, 5 s period) without beam gating and with gating at 30% or 10% of the amplitude and compared with reference data acquired in stationary conditions.

For this test, we used the Apogee Alta U6 (1.05MP, 16bit) CCD. With this camera model, which includes a thermoelectric cooling system, it was possible to acquire long exposure images, one per field, integrating the charge for the duration of each delivery. The 24 μm CCD pixel size, together with a 50 mm focal length, results in 0.313 mm resolution on the scintillating screen.

2.4.4 Test 4 – End-to-end test

Finally, the entire workflow including imaging for planning and patient positioning, up to the treatment delivery has been tested in clinical settings, using an anthropomorphic breathing phantom (Fig. 2c) [29,30]. Two Gafchromic^{TM} EBT3 films (Ashland ISP Advanced Materials, NJ, USA) were inserted proximally and distally along the beam direction in a cylindrical target holder, that moves in the right lung of the phantom. Motion was monitored using two markers on the thorax surface, one caudal close to the umbilicus and one cranial, approximately at the xiphoid. A planning gated-CT at 30% of surface motion amplitude has been used to optimise two posterior SFUD fields (1 Gy (RBE) each) to deliver a homogeneous dose cube (∼17 cc) distribution with 2× volumetric rescanning (Fig. 3 – right panel). Following our clinical protocol, a gated-CT acquired at 30% end-exhale was used to verify the phantom positioning against the planning images. A simplified motion scenario obtained by ventilating the lung with a regular pressure curve following a $sin^4(t)$ and 4 s period has been compared to the realistic case of an irregular breather.

2.5 Quality Assurance program

The Quality Assurance (QA) program is based on the AAPM recommendations for non-radiographic localization and positioning systems [31], adapted to the specific context of proton therapy and internal safety guidelines. A detailed test list and thresholds for tolerance and action levels are summarised in Table 1.

Being a non-permanent installation, anytime the sensor is mounted on the treatment couch it is verified for geometric calibration and accuracy in relative measurements of stationary points (QA-I). The root mean square (RMS) error in the localisation of four markers fixed on a qualified phantom is considered as a figure of merit. Spatial and temporal accuracy in dynamic tracking is assessed on a monthly basis with the test QA-II. A sinusoidal motion is tracked over 10 min and the

Table 1
Summary of quality assurance tests and frequency.

Test	Periodicity	Purpose	Description	Tolerance	Action
QA-I	Daily	Static measurements	Patient localization and monitoring system calibration	NA	1 mm RMSE
QA-II	Monthly	Dynamic measurements	Patient localization and monitoring system: dynamic measurement accuracy	±1 mm 100 ms	±2 mm 200 ms
QA-III	Yearly	Stability (drift/reproducibility)	Patient localization and monitoring system position measurement drift	<0.5 mm/h	<1 mm/h
QA-IV	Yearly	Dynamic gating delivery	Gating delivery dose consistency	γ (2,2) = 95%	γ (2,2) = 90%
QA-V	Yearly	BGMI safety	Functionality of machine interface for beam gating	NA	Functional
QA-VI	Yearly	BGMI TCS Safety	Machine interface for beam gating – special functions	NA	Functional
QA-VII	Yearly	BGMI power supervision	Power supply supervision of BGMI	NA	Functional

recorded signal processed to evaluate discrepancies against nominal amplitude and period values. More specifically, we track 2 cm vertical motion of the QUASAR^{TM} moving platform programmed to run a sinusoidal breathing curve with 5 s period. Yearly tests QA-V, QA-VI and QA-VII are in place to verify the functionality of the BGMI and gating related TCS routines that are specific of our institute. In addition, the commissioning *Test 3*, designed to evaluate the gating system performance on transmission images, is also repeated with yearly frequency as QA-IV. Finally, the stability of position measurement over 1 h of acquisition due to thermal drift of the optical tracker is evaluated and compared to reference values acquired at time of commissioning (QA-III). Following our internal regulations, tests with results out of tolerance are kept under particular observation, exceeding the action level requires instead the immediate termination of clinical treatments and risk assessment from qualified personnel.

3 Results

3.1 Water equivalent thickness of body markers

Water equivalent thickness (WET) of body markers has been estimated for a vertical projection. The complex marker geometry is reflected in the inhomogeneous range change visible in Fig. 4. Maximal values are measured in the central region, where the base plate adds on the sphere holder reaching up to 8 mm WET.

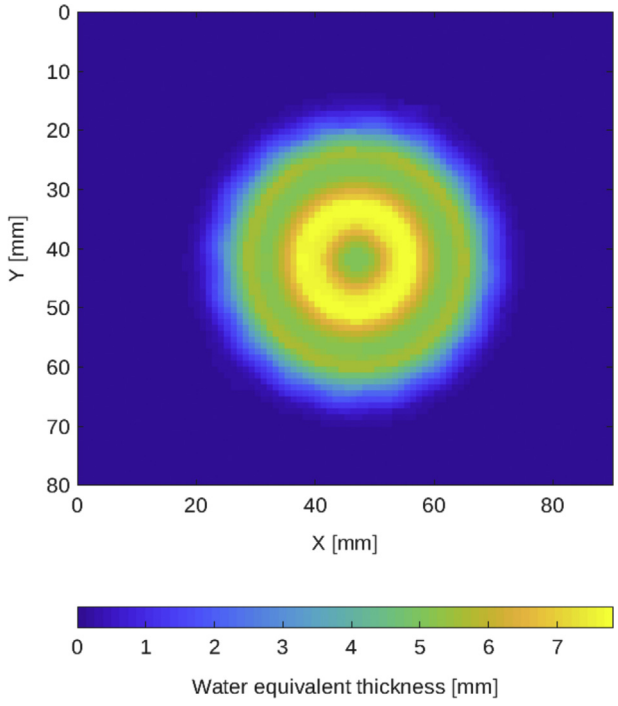

Figure 4. Water equivalent thickness of an optical surface marker estimated from proton radiography data. Note the color-wash scale in millimeter of water.

3.2 Clinical commissioning results

3.2.1 Test 1 – Integrity of dose delivery

In the central region of the field, homogeneous 0.22 Gy and 0.32 Gy were measured respectively at approximately 2 cm and 6 cm water-equivalent depths. No significant difference was observed in the integral dose measured at isocentre with the introduction of beam gating. The gamma pass rates at 1%/1 mm γ(1,1) [32] with respect to reference data acquired without gating were consistently above 99% for all analysed dataset. Similarly, the maximal standard deviation in repeated measurements of dose diagonal profiles across the square field was no more than 0.15 cGy.

3.2.2 Test 2 – Gating effectiveness

The large treatment field optimised for the mediastinal case was only marginally influenced by a small motion amplitude of 5 mm, with a high γ(3,3) pass-rate achieved even without the adoption of specific mitigation techniques (Fig. 5a, b). Using stricter criteria at γ(1,1) however shows how dose

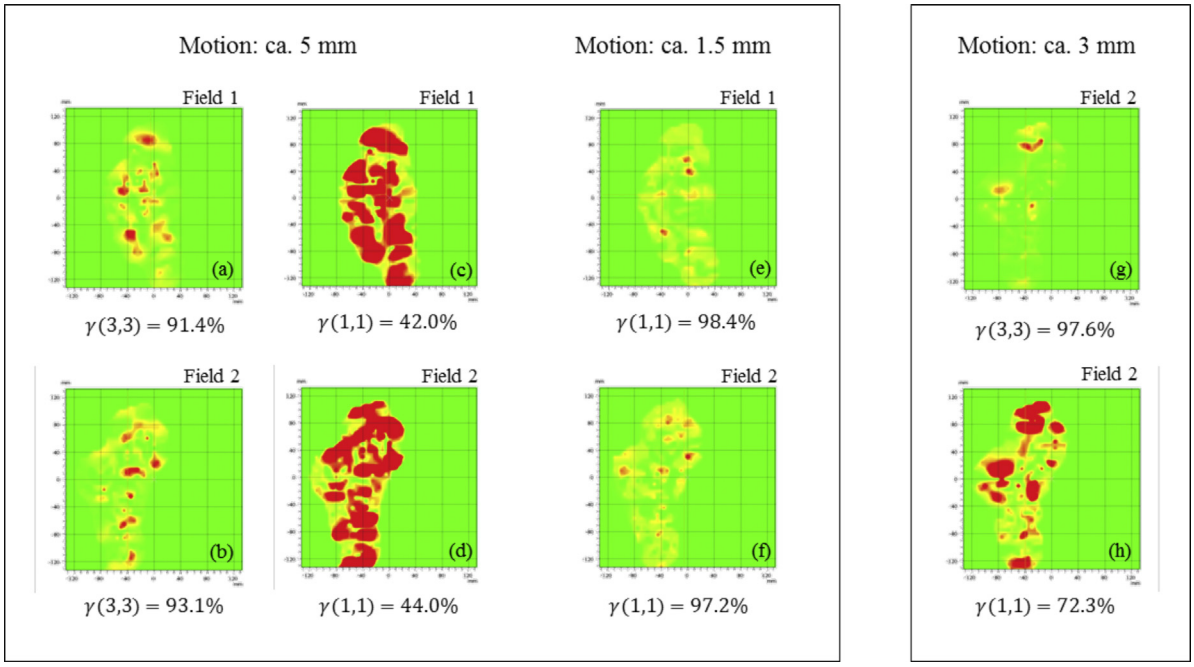

Figure 5. Effectiveness of gating as a function of the residual motion in the treatment window for two proton fields. Results are compared with reference data taken in stationary conditions. Gamma (γ) pass rate at (3%, 3 mm) and (1%, 1 mm) are shown for the worst-case scenario of 5 mm target motion treated without motion-mitigation respectively in (a, b) and (c, d). Dose distortions are controlled with respiratory gating at 30% of the amplitude (e, f) but increase as target motion becomes larger (g, h).

distortions, although subtle, were present (c, d) and can be effectively mitigated by gating the beam around end-exhale phases (e, f). Doubling the target displacement from 5 mm to 10 mm increased the residual motion in the gating window up to 3 mm, with noticeable impact on dose homogeneity (g). Even in this case, however, γ(3,3) was well above 95% (h).

3.2.3 Test 3 – Latency and geometric precision

The overall system performance and reproducibility has been evaluated with high accuracy analysing the transmission images of an absorbing block. The original radiographic shadow with sharp edges created by the object when kept stationary (Fig. 6a), was blurred under the condition of motion (b). Introducing gating recovered the dose distribution captured for the stationary situation gradually for progressively smaller windows (c, d). Achieved γ(2,2) scores for the 10% and 20% gating windows were 96% and 86%, respectively. Two repeated measurements for each window gave reproducible results, passing 1D γ(1,1) across the full profile along the motion direction (Fig. 6, right panel).

3.2.4 Test 4 – End-to-end test

The geometric accuracy in dose localisation for gated treatments was evaluated under realistic clinical settings making use of an anthropomorphic breathing phantom. Depending on the ventilator settings, either $sin^{\$}(t)$ or patient-like breathing patterns, the lung target moved respectively 6 mm and 14 mm, as measured on 4DCT images. The treatment fields were delivered using end-exhale 30% amplitude gating. Assuming good phantom reproducibility, positioning and setup verification was originally based on bony anatomy, for best alignment of the spine. This approach however has lately proven to be incorrect, as the phantom was affected by significant shift in the baseline of the target motion, leading to systematic target misalignment of 2.8 mm and 7.4 mm in cranio-caudal direction for the two ventilating schemes respectively. Such setup corrections for target-based alignment were recalculated *a posteriori* analysing the positioning images and considered when processing the Gafchromic film data. γ(3,3) were 99.6% and 98.6% respectively for the posterior and anterior planes for the sinusoidal regular breathing when compared to the planned distributions. Slightly lower pass rates of 92.9% and 94.3% were measured for the irregular patient respiratory pattern. The same trend can be observed for the dose profiles along the target motion direction, shown in Fig. 7.

3.3 Early results from Quality Assurance tests

The clinical commissioning of the gating procedure started in August 2019 and ran until December of the same year. Since then, the geometry calibration and accuracy in static measurements has been verified 18 times, according to our program for QA-I. On this early dataset, the RMS error

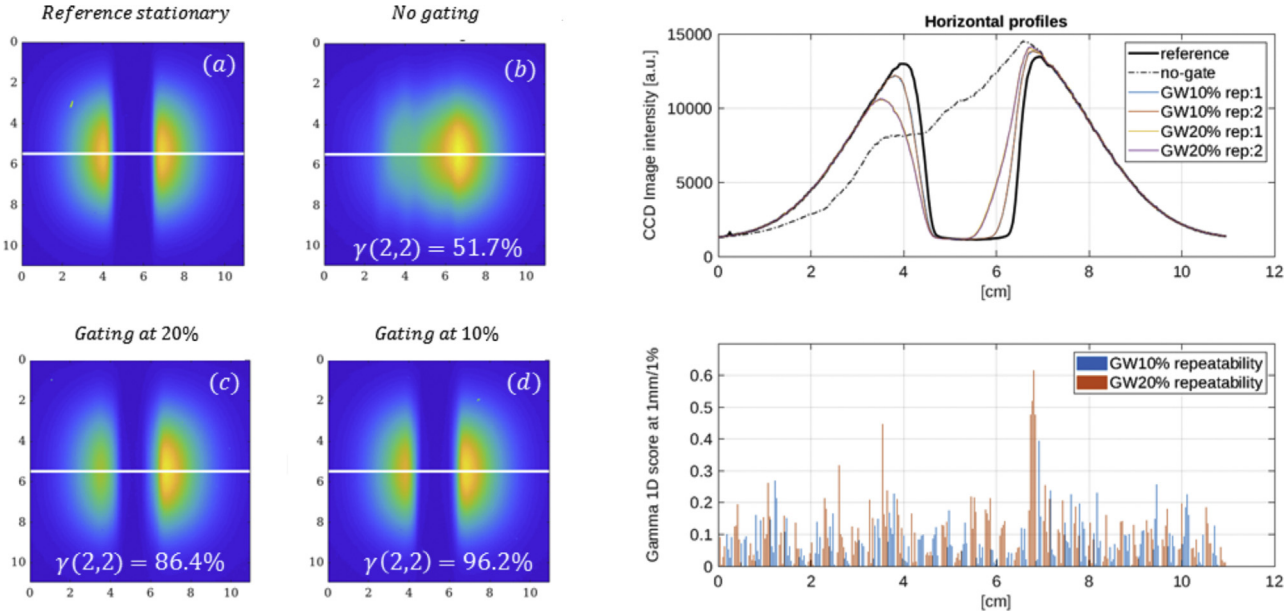

Figure 6. Proton transmission imaging of a 3 × 2 cm thick rod of polyethylene. Reference images acquired in stationary conditions (a) are compared with results under the condition of motions without beam gating (b) and for two window levels at 20% (c) and 10% (d) of the target motion. Horizontal profiles in the middle of the field (white line) are shown for the two test repetitions on the right panel. Gamma 1D score between the two repetitions for each gating window settings are shown at 1 mm/1%.

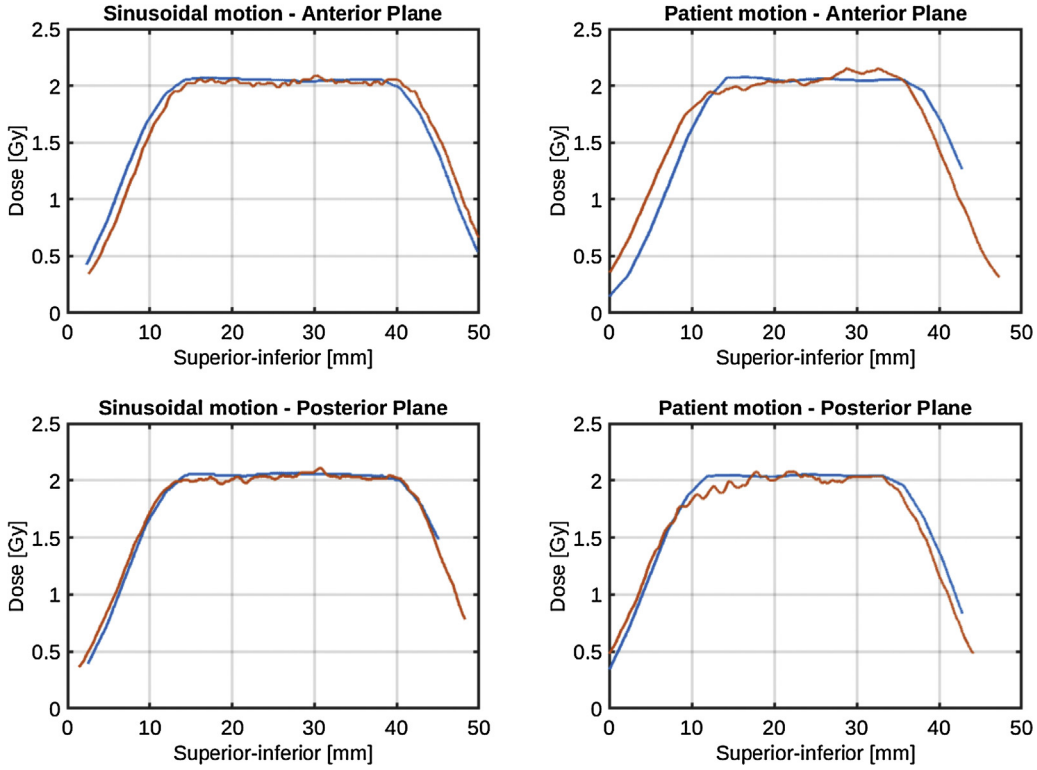

Figure 7. Dose profiles on Gafchromic films at two coronal planes in the target (orange line). Results are compared with planned dose profiles shown in blue for two motion scenarios, sinusoidal regular motion and irregular patient waveform.

in stationary localisation was 0.45 ± 0.04 mm. Dynamic tracking accuracy (QA-II) has been checked with monthly periodicity. We report 0.4 mm and 12.71 ms maximal breathing amplitude and period discrepancy from reference values in three measurements, including the commissioning data. Thermal drift (QA-III) has been quantified at the time of commissioning for two systems available on-site. We have observed considerable variability between the devices, one capable of obtaining stable measurements just after the warming up period (2 min), the other taking about 28 min.

4 Discussion

We have described the integration of a new respiratory gating system in our clinical practice of proton therapy with pencil beam scanning treating patients with moving targets. The tests and methodologies introduced have general validity and cover different medical physics aspects to be considered for the commissioning of a gating system. Similarly, the quality control program is not specific to our implementation and can be applied to other motion monitoring solutions based on optical tracking.

Some RPM installations use NDI tracking technology and, even though it is not a common setup, Polaris Spectra can be found in TrueBeam radiotherapy units. Despite the specific camera hardware however, a key difference is in the approach used to track the breathing motion. RPM measures the displacement of a so-called 'marker block' as a single surrogate of the breathing motion. Several reflective dots (2–6) are required for the localisation of the block, but do not provide independent signals. We use the optical tracking differently, to track the motion of individual markers in a configuration spread across the thoraco-abdominal surface.

The system requires the application of reflective markers on the patient, distributed in a configuration of points on the chest and abdomen. Like any other object that can fall into the treatment field, we have quantified the equivalent range in water to evaluate the potential impact on dose distribution in the patient. With up to about 8 mm of WET in the vertical projection, we consider not advisable to have markers of this type in the beam path, which should therefore be positioned appropriately already at the time of the treatment simulation. Being a system based on multiple redundant markers, this has limited impact on its functionality to monitor respiratory motion. The referring medical doctor and medical physicists define the marker configuration a-priori, before the acquisition of the prospectively gated planning CT. Their decision is based on the clinical experience and any available imaging that provides information about the target location, together with the likely beam arrangement to be used. The recommendation of having at least one ventral and one thoracic marker can be adapted to the individual patients' characteristics, tumour location and related uncertainties. In addition, several different types of optical infrared-reflective markers are available on the market that could have potentially less influence on the treatment.

The first of the commissioning tests (*Test 1*) confirmed that the repeated interruption of treatment based on the gating signal does not affect the total dose delivered. The measurement was carried out in the plateau of a low-dose monoenergetic field, a particularly critical condition that has been preferred to clinical treatment fields to emphasise the impact of even small dose errors. The negligible discrepancies measured between the deliveries with and without gating, as well as the differences of just few cGy on the distribution profiles, are within the reproducibility of the reference dosimeter and not attributable to delivery problems.

The mediastinum treatment plan is an exemplary case close to clinical practice, where tight constraints in scan range often requires the use of progressive patches to cover extended tumour volumes. The *Test 2* setup replicates what could be the method for patient-specific plan verification using a mobile platform. The reported $\gamma(3,3)$ pass rates above 95%, which we consider clinically acceptable, confirm the functionality of the couch-mounted system, even when it moves during the delivery of the treatment. It should be noted that this test does not only verify the gating technology integration but is a comprehensive evaluation of motion mitigation by respiratory gating.

Test 3 was designed to evaluate systematic latencies of the gating system and its reproducibility in dose delivery control. Keeping the detector stationary with the QUASAR^{TM} on top is important to ensure repeatable measurement conditions, unaffected by the inaccuracies of movement that occur when the mobile platform is loaded with weight. For this test, we used a square mono-energetic field where all spots are weighted equally. In our implementation, where the single spot is not interrupted except for safety reasons, that is expected to limit the uncertainty in the dose delivered outside the gating window to the same, fixed, maximal spot duration. The test proved to be a sensitive method to evaluate the performance of the gating system and showed that, if the gating window is small enough, it is possible to recover the measured dose distribution under stationary conditions. The profile analysis showed excellent reproducibility of the system, sub-millimetre inaccuracies in the position of the radiographic shadow are in agreement with the movement accuracy of the QUASAR^{TM} platform and the CCD resolution.

The end-to-end test performed with an anthropomorphic phantom is a comprehensive test of the clinical workflow, with focus on imaging and patient positioning components. The phantom materials, however, are not tissue equivalent and do not lie exactly on the Hounsfield unit to relative stopping power calibration curve, so we do not expect a perfect match with the dose distribution calculated in the planning system. The baseline target shift, not accounted for by phantom positioning based on bony anatomy, resulted in a geometrical shift in the measured dose in the target. Nevertheless, the geometric error on the film was in agreement with the

baseline shift observed retrospectively on the positioning images when performing a target-based alignment. This is a confirmation that the setup could be well controlled following the described workflow, and therefore the known baseline drift has been accounted for while processing the results. Repositioning errors of optical markers and inter-fractional changes in the internal/external correlation, typical issues of gating systems based on external surrogates, are mitigated by positioning the patient with a CT gated in the same breathing window used for treatment. Observed differences in dose profiles were in the order of millimetres, compatible with the accuracy of the measurement process, which relied on 2 mm slice thickness planning images.

Thermal drift is known to affect optical tracking systems and is device dependent. It is therefore not surprising to observe large variations even between devices of the same model type as in our case. Even though its parametrisation is possible, we have decided for the easiest solution to ensure reliable tracking during clinical operations, i.e. powering up the device well in advance, if not leaving it always on.

QA test results were always within the specified tolerances. Although the dataset is currently too limited to draw definitive conclusions, the small variance observed in static and dynamic QA measurements bodes well for the reproducibility of the system in the long term.

5 Conclusions

We have presented the commissioning of a novel solution for respiratory-gated proton therapy based on optical tracking of surface markers. The tests described, relying on equipment typically available in radiotherapy departments, can be replicated in other facilities and may serve as a guideline for the clinical integration of technologies for motion mitigation. In addition, periodical quality assurance tests are provided specifically to the use of optical technologies for real-time breathing monitoring. The dosimetric results in simplified geometries and realistic clinical conditions confirmed the correct interaction of our gating system with the therapy control system and the imaging devices. Following this successful commissioning and QA program, the system has been successfully validated for clinical use in our institute.

Authors' contributions

GF, SS, JH, TL, MW, DCW defined the requirements specifications of the system. GF, HR, CB, SD, AM, UR, DO, RV, DL led the development of hardware and software technologies. MG, GF assessed the risks associated with the use of gating. GF, SS, TL, DCW defined and approved the QA program. GF, JH, SS, AB, TL defined the clinical acceptance and commissioning tests. GF, JH, TB, AB, MT, RV, EC acquired experimental data required for the clinical commissioning. All authors reviewed and approved the final manuscript.

Acknowledgements

The authors acknowledge the radiation therapists and medical physicists of Center for Proton Therapy at Paul Scherrer Institut for their support in the commissioning activities.

References

[1] Bert C, Durante M. Motion in radiotherapy: particle therapy. Phys Med Biol 2011;56(16):R113–44.
[2] Lim PS, Pica A, Hrbacek J, Bachtiary B, Walser M, Lomax AJ, et al. Pencil beam scanning proton therapy for paediatric neuroblastoma with motion mitigation strategy for moving target volumes. Clin Oncol (R Coll Radiol) 2020.
[3] Ciocca M, Mirandola A, Molinelli S, Russo S, Mastella E, Vai A, et al. Commissioning of the 4-D treatment delivery system for organ motion management in synchrotron-based scanning ion beams. Phys Med 2016;32(12):1667–71.
[4] Meschini G, Seregni M, Pella A, Ciocca M, Fossati P, Valvo F, et al. Evaluation of residual abdominal tumour motion in carbon ion gated treatments through respiratory motion modelling. Phys Med 2017;34:28–37.
[5] Bertholet J, Knopf A, Eiben B, McClelland J, Grimwood A, Harris E, et al. Real-time intrafraction motion monitoring in external beam radiotherapy. Phys Med Biol 2019;64(15), 15TR01–34.
[6] Li XA, Stepaniak C, Gore E. Technical and dosimetric aspects of respiratory gating using a pressure-sensor motion monitoring system. Med Phys 2005;33(1):145–54.
[7] Steidl P, Haberer T, Durante M, Bert C. Gating delays for two respiratory motion sensors in scanned particle radiation therapy. Phys Med Biol 2013;58(21):N295–302.
[8] Minohara S, Kanai T, Endo M, Noda K, Kanazawa M. Respiratory gated irradiation system for heavy-ion radiotherapy. Radiat Oncol Biol 2000;47(4):1097–103.
[9] Lu H-M, Brett R, Sharp G, Safai S, Jiang S, Flanz J, et al. A respiratory-gated treatment system for proton therapy. Med Phys 2007;34(8):3273–8.
[10] Gelover E, Deisher AJ, Herman MG, Johnson JE, Kruse JJ, Tryggestad EJ. Clinical implementation of respiratory-gated spot-scanning proton therapy: an efficiency analysis of active motion management. J Appl Clin Med Phys 2019;20(5):99–108.
[11] Franz AM, Haidegger T, Birkfellner W, Cleary K, Peters TM, Maier-Hein L. Electromagnetic tracking in medicine – a review of technology, validation, and applications. IEEE Trans Med Imaging 2014;33(8):1702–25.
[12] Fattori G, Safai S, Carmona PF, Peroni M, Perrin R, Weber DC, et al. Monitoring of breathing motion in image-guided PBS proton therapy: comparative analysis of optical and electromagnetic technologies. Radiat Oncol 2017;12(1):63.
[13] Shi C, Tang X, Chan M. Evaluation of the new respiratory gating system. Prec Radiat Oncol 2017;1(4):127–33.
[14] Hoisak JDP, Pawlicki T. The role of optical surface imaging systems in radiation therapy. Semin Radiat Oncol 2018;28(3):185–93.
[15] Baroni G, Riboldi M, Spadea MF, Tagaste B, Garibaldi C, Orecchia R, et al. Integration of enhanced optical tracking techniques and imaging in IGRT. J Radiat Res 2007;48(Suppl. A):A61–74.
[16] Ricotti R, Ciardo D, Fattori G, Leonardi MC, Morra A, Dicuonzo S, et al. Intra-fraction respiratory motion and baseline drift during breast Helical Tomotherapy. Radiother Oncol 2017;122(1):79–86.
[17] Gianoli C, Riboldi M, Spadea MF, Travaini LL, Ferrari M, Mei R, et al. A multiple points method for 4D CT image sorting. Med Phys 2011;38(2):656–67.
[18] Cala SJ, Kenyon CM, Ferrigno G, Carnevali P, Aliverti A, Pedotti A, et al. Chest wall and lung volume estimation by optical reflectance motion analysis. J Appl Physiol 1996;81(6):2680–9.

[19] Seregni M, Kaderka R, Fattori G, Riboldi M, Pella A, Constantinescu A, et al. Tumor tracking based on correlation models in scanned ion beam therapy: an experimental study. Phys Med Biol 2013;58(13):4659–78.
[20] Bert C, Metheany KG, Doppke K, Chen GTY. A phantom evaluation of a stereo-vision surface imaging system for radiotherapy patient setup. Med Phys 2005;32(9):2753–62.
[21] Fattori G, Riboldi M, Desplanques M, Tagaste B, Pella A, Orecchia R, et al. Automated fiducial localization in CT images based on surface processing and geometrical prior knowledge for radiotherapy applications. IEEE Trans Biomed Eng 2012;59(8):21919.
[22] Pella A, Riboldi M, Tagaste B, Bianculli D, Desplanques M, Fontana G, et al. Commissioning and quality assurance of an integrated system for patient positioning and setup verification in particle therapy. Technol Cancer Res Treat 2014;13(4):303–14.
[23] Fattori G, Saito N, Seregni M, Kaderka R, Pella A, Constantinescu A, et al. Commissioning of an integrated platform for time-resolved treatment delivery in scanned ion beam therapy by means of optical motion monitoring. Technol Cancer Res Treat 2014;(6):517–28.
[24] Fattori G, Seregni M, Pella A, Riboldi M, Capasso L, Donetti M, et al. Real-time optical tracking for motion compensated irradiation with scanned particle beams at CNAO. Nuclear Inst and Methods Phys Res A 2016;827(C):39–45.
[25] Riboldi M, Orecchia R, Baroni G. Real-time tumour tracking in particle therapy: technological developments and future perspectives. Lancet Oncol 2012;13(9):e383–91.
[26] Zenklusen SM, Pedroni E, Meer D. A study on repainting strategies for treating moderately moving targets with proton pencil beam scanning at the new Gantry 2 at PSI. Phys Med Biol 2010;55(17):21–5103.
[27] Pedroni E, Bearpark R, Böhringer T, Coray A, Duppich J, Forss S, et al. Gantry 2: a second generation proton scanning gantry. Zeitschrift für Medizinische Physik 2014;14(1):25–34.
[28] Boon SN, van Luijk P, Böhringer T, Coray A, Lomax A, Pedroni E, et al. Performance of a fluorescent screen and CCD camera as a two-dimensional dosimetry system for dynamic treatment techniques. Med Phys 2000;27(10):208–198.
[29] Perrin RL, Zakova M, Peroni M, Bernatowicz K, Bikis C, Knopf AK, et al. An anthropomorphic breathing phantom of the thorax for testing new motion mitigation techniques for pencil beam scanning proton therapy. Phys Med Biol 2017;62(6):504–2486.
[30] Colvill E, Krieger M, Bosshard P, Steinacher P, Rohrer Schnidrig BA, Parkel T, et al. Anthropomorphic phantom for deformable lung and liver CT and MR imaging for radiotherapy. Phys Med Biol 2020;65(7), 07NT02.
[31] Willoughby T, Lehmann J, Bencomo JA, Jani SK, Santanam L, Sethi A, et al. Quality assurance for nonradiographic radiotherapy localization and positioning systems: Report of Task Group 147. Med Phys 2012;39(4):1728–47.
[32] Low DA, Harms WB, Mutic S, Purdy JA. A technique for the quantitative evaluation of dose distributions. Med Phys 1998;25(5):656–61.